ISSN 1063-7834, Physics of the Solid State, 2011, Vol. 53, No. 3, pp. 654–664. © Pleiades Publishing, Ltd., 2011.
Original Russian Text © S.Yu. Davydov, G.I. Sabirova, 2011, published in Fizika Tverdogo Tela, 2011, Vol. 53, No. 3, pp. 608–616.

GRAPHENES

Model of Adsorption on Graphene

S. Yu. Davydov[a, *] and G. I. Sabirova[b]

[a] *Ioffe Physical-Technical Institute, Russian Academy of Sciences, Politekhnicheskaya ul. 26, St. Petersburg, 194021 Russia*
** e-mail: Sergei_Davydov@mail.ru*

[b] *St. Petersburg State Electrotechnical University "LETI," ul. Professora Popova 5a, St. Petersburg, 197022 Russia*

Received June 28, 2010

Abstract—A simple *M*-shaped model has been proposed for the density of states of the π bands of the graphene. The model has been used to derive the expression for the local density of states on the adsorbed atom and to calculate the corresponding occupation numbers for different model parameters. Additional simplifications have made it possible to represent the band contribution n_b to the total occupation number of the adatom n_a in the analytical form. The contributions of local states n_l to $n_a = n_b + n_l$ have been calculated for different parameters. The charge has been numerically evaluated for the case of adsorption of alkali metal atoms on the graphene. The results obtained have been verified using the model of a surface diatomic molecule calculated by the Harrison bond-orbital method. The verification has demonstrated that the charges calculated in terms of radically different models are in good agreement.

DOI: 10.1134/S1063783411030061

1. INTRODUCTION

In recent years, the adsorption properties of carbon nanostructures have attracted stable interest of researchers [1–4]. This is not surprising because the elucidation of mechanisms of the interaction between a foreign atom and a carbon structure is important from the fundamental point of view (charge transfer, carrier scattering, and surface magnetism) and the applied standpoint (doping, passivation, and sensorics). For nanostructures, the study of adsorption is especially valuable because the role of the surface with respect to the volume in these objects is significant. Actually, if the characteristic linear size of the system is L, the ratio between its surface area proportional to L^2 and the volume proportional to L^3 increases with a decrease in L.

With the advent of the graphene [5, 6], i.e., the two-dimensional hexagonal lattice formed by carbon atoms, the investigations of the adsorption properties have been extended to this new structure. Owing to the simplicity of the structure, the graphene is an ideal object for theoretical studies, whereas the situation from the experimental viewpoint is not so simple: the graphene should be fixed in space in a particular manner without significant disturbance of its two-dimensionality. Therefore, it is not surprising that the number of theoretical works concerning the adsorption on the graphene progressively increases (see, for example, [6–15] and references therein) and exceeds experimental investigations [16–20] (see also references to earlier works in these publications) by one order of magnitude. It should be noted that, in the majority of cases, the calculations have been carried out using the density functional theory [6, 9, 10, 14, 15].

As a result of the performed investigations, it has been possible to generally establish the main characteristics of adsorption of particles of different natures (alkali metals, gases, halogens, hydrogen): the location of adsorption centers, the nature of the bonding between adparticle and substrate, the charge transfer between them, and changes in the electronic structure of graphene due to adsorption. It is especially interesting to note that, at a specific concentration of adatoms, gaps absent before adsorption can appear in the electronic spectrum of graphene. Moreover, there can appear a gap in the total density of states of the single-layer graphene.

Apart from numerical calculations in the framework of the density functional theory or other schemes, there exists a model approach to the adsorption problem. The pioneer of this approach was Newns [21], who used the Anderson Hamiltonian [22] for describing the adsorption on metals (see also [23–25]). Subsequently, this approach was generalized to the case of semiconductor substrates (Haldane–Anderson model [26, 27], see also the description of the adsorption on semiconductors in terms of the Anderson model [28–30]) and graphite [31, 32]. In the present paper, we propose a model of the density of states of the graphene that allows one to represent of the density of states on an adatom in the analytical form. Furthermore, by using a number of sufficiently clear simplifications, we succeeded in deriving the

explicit expression for the occupation number of the adatom and, consequently, its charge.

2. MODEL OF THE DENSITY OF STATES OF THE GRAPHENE AND THE DENSITY OF STATES ON THE ADATOM

The Hamiltonian of the problem H is written in the form of the Haldane–Anderson Hamiltonian [26, 27]

$$H = \sum_{k\sigma} \varepsilon_k c_{k\sigma}^+ c_{k\sigma} + \varepsilon_a \sum_{\sigma} a_\sigma^+ a_\sigma + U a_\uparrow^+ a_\uparrow a_\downarrow^+ a_\downarrow + N^{-1/2} \sum_{k\sigma} (V_{ka} c_{k\sigma}^+ a_\sigma + \text{h.c.}). \quad (1)$$

Here, ε_k is the band energy of a substrate electron in the state $|k\sigma\rangle$ (as in [26, 27], the band index is omitted), ε_a is the energy of an atomic electron in the state $|a\sigma\rangle$, U is the intra-atomic Coulomb repulsion of electrons with opposite spins σ, i.e., in the states $|a\uparrow\rangle$ and $|a\downarrow\rangle$ on the adatom, V_{ka} is the matrix element of hybridization of the states $|k\sigma\rangle$ and $|a\sigma\rangle$, $c_{k\sigma}^+(c_{k\sigma})$ are the creation (annihilation) operators of the electron in the state $|k\sigma\rangle$, $a_\sigma^+(a_\sigma)$ are the corresponding operators of the electron in the state $|a\sigma\rangle$, h.c. stands for the Hermitian conjugate terms, and N is the number of atoms of the graphene. In the extended Hartree–Fock approximation, Hamiltonian (1) corresponds to the Green's function of the adatom in the form

$$G_{a\sigma}^- = \omega - \varepsilon_{a\sigma} - \Lambda(\omega) + i\Gamma(\omega), \quad (2)$$

where

$$\varepsilon_{a\sigma} = \varepsilon_a + U n_{a-\sigma}, \quad n_{a\sigma} = \langle a_\sigma^+ a_\sigma \rangle, \quad (3)$$

$$\Gamma(\omega) = \pi V^2 N^{-1} \sum_k \delta(\omega - \varepsilon_k), \quad (4)$$

$$\Lambda(\omega) = \frac{1}{\pi} P \int_{-\infty}^{\infty} \frac{\Gamma(\omega')}{\omega - \omega'} d\omega'. \quad (5)$$

In relationships (2)–(5), ω stands for the energy variable; $n_{a\sigma}$ is the occupation number for the state of the adsorbed atom (adatom) $|a\sigma\rangle$; $\langle ... \rangle$ is the averaging over the ground state; $\delta(...)$ is the Dirac delta function; P is the symbol of the principal value; and Γ and Λ are the half-width and the hybridization shift of the adatom's quasilevel, respectively. In expression (4) and below, we ignore the k dependence of the matrix element V_{ka}.

Since the energy density of states of the graphene (per atom) is $\rho_g(\omega) = N^{-1} \sum_k \delta(\omega - \varepsilon_k)$, we can write

$$\Gamma(\omega) = \pi V^2 \rho_g(\omega) \quad (6)$$

instead of Eq. (4). Therefore, by specifying the substrate density of states of the and using relationships (6) and (5), we can find the Green's function (2). This is the essence of the model approach to the problem of adsorption. In particular, the advantage of this approach is the possibility of obtaining analytical results, whereas the use of the density functional theory requires the performance of numerical calculations in each specific case.

In order to specify the graphene density of states, it is necessary to carry out the corresponding calculations of the dispersion of the π and π^* bands formed by bonding and antibonding combinations of the p_z orbitals of neighboring carbon atoms (we assume that the graphene lies in the $(x, y, 0)$ plane). As is known, the graphene can be treated as a limiting case of graphite when the interaction between hexagonal planes can be disregarded. This circumstance played its positive role, because it is this approximation that was used as a zeroth approximation in the calculations of the band structure of graphite in earlier works [33–36]. According to the results obtained in [6, 34, 37, 38], the density of states of the graphene $\rho_g(\omega)$ (per atom) can be represented in the form

$$\rho_g(\omega) = \begin{cases} 0, & \omega < -D/2 \\ -\dfrac{\rho_m \Delta}{2\omega}, & -D/2 < \omega < -\Delta/2 \\ \dfrac{2\rho_m |\omega|}{\Delta}, & -\Delta/2 < \omega < \Delta/2 \\ \dfrac{\rho_m \Delta}{2\omega}, & \Delta/2 < \omega < D/2 \\ 0, & \omega > D/2. \end{cases} \quad (7)$$

Here, $D/2$ is the width of the π and π^* bands of the graphene that lie below and above $\omega = 0$, respectively, where zero energy corresponds to the Dirac point K in the Brillouin zone, and Δ is the width of the "pseudogap." We introduce the dimensionless density of states $f(x) = \rho_g(x)/\rho_m$, where $x = 2\omega/\Delta$ and $D/\Delta = d$. The dependence $f(x)$ is plotted in Fig. 1, where $d = 3$ [33, 34, 37]. It should be noted that, in the ordered two-dimensional structure, the divergence (Van Hove singularity) occurs at the points $\omega = \pm\Delta/2$, where $\rho_g(\omega) \longrightarrow \infty$. However, we cut the graph $\rho_g(\omega)$ by setting $\rho_g(\pm\Delta/2) = \rho_m$. The quantity ρ_m (per atom) can be easily determined from the normalization taking into account that the free p_z orbital of graphene atom contains one electron. As a result, we obtain

$$\rho_m = \frac{4}{1 + 2\ln d} \frac{1}{\Delta}. \quad (8)$$

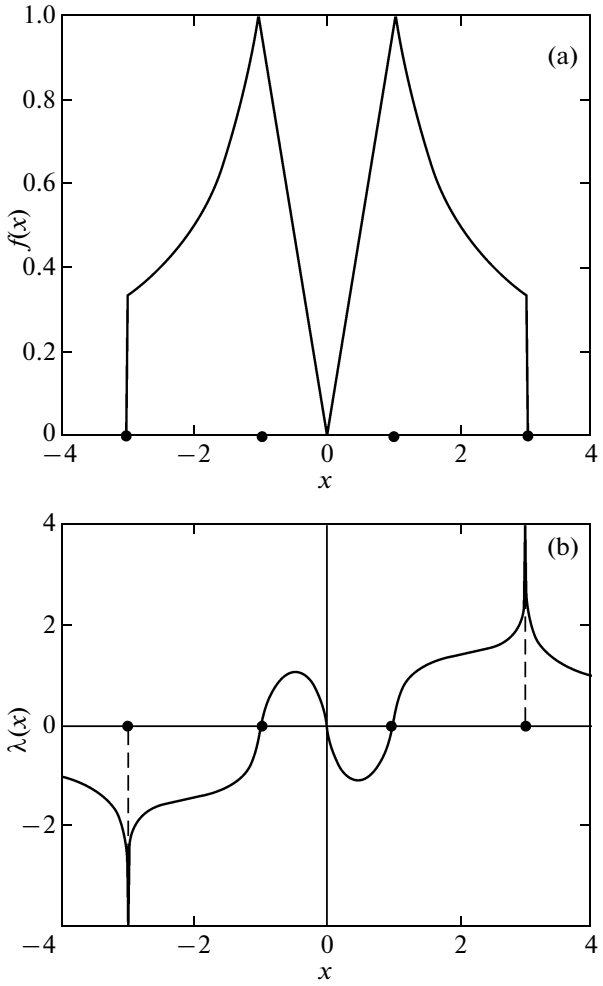

Fig. 1. Dependences of (a) the reduced density of states of the graphene $f = \rho_g/\rho_m$ and (b) the reduced shift function of the level of the adatom $\lambda = \Lambda/\rho_m V^2$ on the dimensionless energy $x = 2\omega/\Delta$.

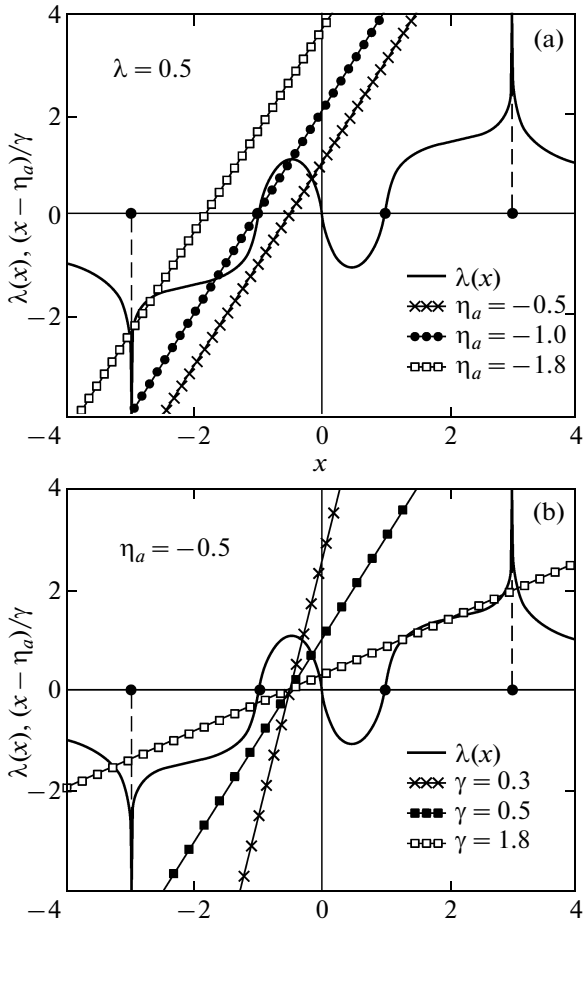

Fig. 2. Graphical solution of the equation $x - \eta_a - \gamma\lambda(x) = 0$ (Eq. (13)) for (a) $\gamma = 0.5$ and $\eta_a = -0.5$, -1.0, and -1.8 and (b) $\eta_a = -0.5$ and $\gamma = 0.3$, 0.5, and 1.8. Straight lines correspond to the functions $(x - \eta_a)/\gamma$.

It should be noted that, below, we will need some characteristics, such as the shift function Λ determined by the integral of $\rho_g(\omega)$ over the energy ω, the occupation number of the adatom, which is calculated as the integral of the corresponding density of states (see below), and the adsorption energy (also integral characteristic). In the calculations of these integral parameters, the inaccuracies in the simulation of the density of states $\rho_g(\omega)$ are smoothed.

The local adatom's density of states is $\rho_{a\sigma}(\omega) = -\pi^{-1}\mathrm{Im}G_{a\sigma}$, which gives with (3) in mind the Lorenian form

$$\rho_{a\sigma}(\omega) = \frac{1}{\pi}\frac{\Gamma(\omega)}{(\omega - \varepsilon_{a\sigma} - \Lambda(\omega))^2 + \Gamma(\omega)^2}. \qquad (9)$$

Now, we find the explicit form of the shift function of the level of the adatom $\Lambda(\omega)$ with the use of relationships (5) and (7). As a result, we have

$$\lambda(x) = x\ln\left|\frac{x^2}{1-x^2}\right| + \frac{1}{x}\ln\left|\frac{1-x^2}{1-(x/d)^2}\right|, \qquad (10)$$

where $\lambda(x) = \Lambda(x)/\rho_m V^2$. The dimensionless shift function is shown in Fig. 2. Then, the dimensionless local density of states $\bar{\rho}_{a\sigma}$ on the adatom takes the form

$$\bar{\rho}_{a\sigma}(x) = \rho_{a\sigma}(x)\frac{\Delta}{2} = \frac{1}{\pi}\frac{\pi\gamma f(x)}{(x - \eta_{a\sigma} - \gamma\lambda(x))^2 + (\pi\gamma f(x))^2}, \qquad (11)$$

where $\gamma = 2\rho_m V^2/\Delta$ and $\eta_{a\sigma} = 2\varepsilon_{a\sigma}/\Delta$. Since the function $\lambda(x)(\Lambda(\omega))$ is antisymmetric (Fig. 2), it is easy to show that $\bar{\rho}_a(x, \eta_a) = \bar{\rho}_a(-x, -\eta_a)$.

Let us consider the energies of the local and resonance states induced by the adsorption in the system. These energies are determined by the real poles of the Green's function (2), i.e., by the solutions of the equation

$$\omega - \varepsilon_a - \Lambda(\omega) = 0 \quad (12)$$

or

$$x - \eta_a - \gamma\lambda(x) = 0. \quad (13)$$

Hereafter, we will omit the spin index σ and consider all characteristics for one spin projection.

The graphic solution of Eq. (13) is presented in Fig. 2. In the case of $\gamma = \text{const}$ (Fig. 2a), the shift of the level η_a along the reduced-energy axis x from $-\infty$ to $+\infty$ changes the number of local and resonance levels. In particular, at $\eta_a \ll -3$ ($\varepsilon_a \ll -D/2$), there are two local levels x_{l-} and x_{l+} lying below and above the continuum $(-3, +3)$, respectively: $x_{l-} \sim \eta_a$ and $x_{l+} \sim 3$. There is also one resonance level $x_r \sim 3$ located near the upper edge of the continuum. However, here, it should be noted that the levels $x_{l+} \sim 3$ and $x_r \sim 3$ can be artefacts associated with the divergences of the shift function $\lambda(x)$ at $x = \pm 3$ (Fig. 1b). In turn, these divergences correspond to the jumps in the density of states of the graphene at the above points (Fig. 1a). In a more realistic approximation excluding these jumps, the function $\lambda(x)$ at $x = \pm 3$ would have extrema with a finite magnitude. Then, at $\eta_a \ll -3$, the inequality $(3 - \eta_a)/\gamma > \lambda(3)$ can be satisfied, and, as a result, the levels $x_{l+} \sim 3$ and $x_r \sim 3$ do not arise in the system.

In the shift of η_a toward the range of the continuum $(-3, +3)$, in the system, there can arise five (Fig. 2a, $\eta_a = -1.8$ and -0.5) or seven (Fig. 2a, $\eta_a = -1.0$) levels, of which four (two local and two resonance) levels lie in the vicinity of the lower and upper edges of the density of states, whereas the other (resonance) levels lie in the continuum. At $\eta_a \gg 3$, there arises a situation that specularly reflects the case of $\eta_a \ll -3$: the levels $x_{l-} \sim -3$, $x_r \sim -3$, and $x_{l+} \sim \eta_a$ are observed in the system.

Now, we consider Fig. 2b. At $\eta_a = \text{const}$, an increase in the quantity γ leads to a change in the number of levels in the system: for example, five resonance levels ($\gamma = 1.8$) can be located in the range $(-3, +3)$.

As an example, let us examine some particular cases allowing for analytical solutions. We assume that $|\eta_a| \ll 1$. In this case, it can be seen from Fig. 2 that there exists a resonance level $|x_{r0}| \ll 1$ with the energy that can be evaluated from the approximate equation

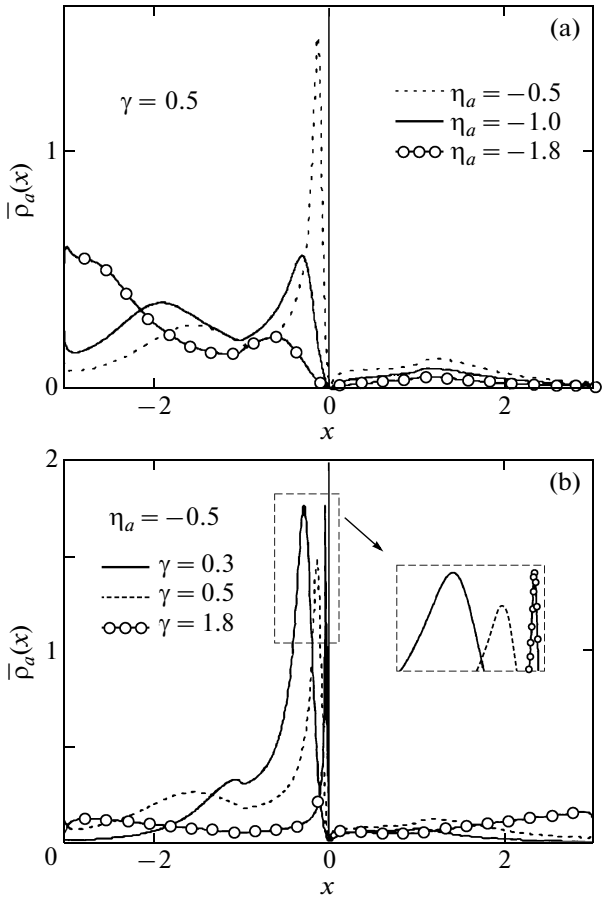

Fig. 3. Reduced local densities of states on the adatom $\bar{\rho}_a(x) = \rho_a(x)\Delta/2$ for (a) $\gamma = 0.5$ and $\eta_a = -0.5$, -1.0, and -1.8 and (b) $\eta_a = -0.5$ and $\gamma = 0.3$, 0.5, and 1.8. The inset shows the mutual location of the maxima of the local density of states for different values of γ on an enlarged scale.

$$\frac{x - \eta_a}{\gamma} \approx 2x\ln|x|.$$

From this equation, we obtain

$$x_{r0} \approx \frac{\eta_a}{1 - 2\gamma\ln|x_{r0}|}. \quad (14)$$

Two more (resonance and local) levels arise at the right ($\eta_a < 0$) or left ($\eta_a > 0$) edges of the density of states. Their energies are written in the form

$$\begin{aligned} x_l^{(2)} &= d\sqrt{1 + \exp(-d/\gamma)}, \\ x_r^{(2)} &= d\sqrt{1 - \exp(-d/\gamma)}, \quad \eta_a < 0, \\ x_l^{(1)} &= -d\sqrt{1 + \exp(-d/\gamma)}, \\ x_r^{(1)} &= -d\sqrt{1 - \exp(-d/\gamma)}, \quad \eta_a > 0. \end{aligned} \quad (15)$$

Now, we analyze the case of $|\eta_a| \gg d$. It can be seen from Fig. 2 that, in this case, there arise two local levels

($x_l' \propto \eta_a$ and $x_l'' \sim \pm d$) and one resonance level lying in the vicinity of the upper ($\eta_a < 0$) or lower ($\eta_a > 0$) edges of the density of states in the system. The energies of these levels are represented by the expressions

$$x_l' = \frac{1}{2}\eta_a[1 + \sqrt{1 + (2\gamma/\eta_a)^2}], \quad (16)$$

$$\begin{aligned} x_l'' &= \pm d\sqrt{1 + \exp(-d|\eta_a|/\gamma)}, \\ x_r &= \pm d\sqrt{1 - \exp(-d|\eta_a|/\gamma)}, \end{aligned} \quad (17)$$

where signs $\pm$ correspond to the cases of $\eta_a < 0$ and $\eta_a > 0$, respectively.

The reduced densities of states on the adatom for different values of the parameters γ and η_a are shown in Fig. 3. Initially, we consider the situation when $\gamma =$ const and the position of the level of the adatom $\eta_a < 0$ is changed (Fig. 3a). The main feature of the density of states is the presence of the central (at the energy x_0) and side (at $x_1 < x_0$) maxima. A comparison of Figs. 3a and 2a indicates that these maxima are associated with the corresponding resonance levels of the system.

When the level of the adatom $\eta_a < 0$ is shifted from the center of the density of states toward its left edge $x = -3$, both maxima shift toward the range of negative energies and their weights are redistributed: the side maximum $\bar{\rho}_a(x_1)$ increases, and the central maximum $\bar{\rho}_a(x_0)$ decreases. It is easy to understand that the shifts in the positions of the maxima at x_0 and x_1 to the left are explained by the increase in $|\eta_a|$ that leads to the shift in the resonance level $x_r = \eta_a + \gamma\lambda(x_r)$ to $x = -3$. A more detailed analysis is given in Appendix 1.

The graphs for $\eta_a = -0.5$ and three different values of the parameter γ are depicted in Fig. 3b. Here, it should be noted that, first, the main maximum $\bar{\rho}_a(x_0)$ located at the point x_0 ($x_0 < 0$ at $\eta < 0$, $|x_0| \ll 1$) is shifted toward the center of the density of states. This behavior of the central maximum can be explained as follows. With an increase in the parameter γ, the position of the shifted level of the adatom $\eta_a'(x_0) = \eta_a + \gamma\lambda(x_0)$ shifts toward zero, because $\eta_a < 0$ and $\lambda(x_0) > 0$. In this case, the quantity $f(x_0)$ decreases and the value of $\bar{\rho}_a(x_0)$ increases. (It should be noted in parentheses that the position x_r determined by the solution of the equation $\eta_a'(x_r) = \eta_a + \gamma\lambda(x_r)$ at small values of $\pi\gamma f(x)$ almost coincides with x_0.) Second, it can be seen from Fig. 3a that an increase in the parameter γ results in a shift of the side maximum $\bar{\rho}_a(x_1)$ toward the left edge of the density of states $x = -3$. This is explained by the fact that the value of $\eta_a'(x_1) = \eta_a + \gamma\lambda(x_1)$ shifts in this direction, because we have $\lambda(x_1) < 0$ and the quantity $|\lambda(x_1)|$ increases with an increase in $|x_1|$. Finally, it should also be noted that the dependence of the main maximum $\bar{\rho}_a(x_0)$ on the parameter γ exhibits a nonmonotonic behavior, which is associated with the shift in the position x_0 and with the specific features of the reduced density of states of the graphene. All these dependences are discussed in more detail in Appendix 1.

3. CHARGE OF THE ADATOM

At zero temperature, the occupation number of the adatom is defined in the conventional manner

$$n_a = \int_{-\infty}^{E_F} \rho_a(\omega)d\omega, \quad (18)$$

where E_F is the Fermi level. Here, we consider the case when the number of electrons on the adatom cannot exceed unity. In the framework of the extended Hartree–Fock theory, the level energies of the adatom for two spin projections are determined by expressions (3). By assuming that the intra-atomic Coulomb repulsion $U \longrightarrow \infty$, we obtain $\varepsilon_{a\uparrow} \approx \varepsilon_a$, $\varepsilon_{a\downarrow} \approx \varepsilon_a + U$, and $n_{a\uparrow} \approx n_a$, $n_{a\downarrow} \approx 0$; i.e., only one spin state is occupied.[1] It is this situation that is examined in our work.

The occupation number is conveniently represented as the sum of the band (n_b) and local (n_l) contributions

$$n_a = n_b + n_l, \quad n_l' = \sum_i n_{li}, \quad (19)$$

where

$$n_b = \int_{-D/2}^{E_F} \rho_a(\omega)d\omega = \int_{-d}^{\varepsilon_F} \bar{\rho}_a(x)dx, \quad (20)$$

$$n_{li} = \left|1 - \frac{\partial\Lambda(\omega)}{\partial\omega}\right|_{\omega_{li}}^{-1} = \left|1 - \gamma\frac{\partial\lambda(x)}{\partial x}\right|_{x_{li}}^{-1}. \quad (21)$$

Here, $\varepsilon_F = 2E_F/\Delta$ is the reduced value of the Fermi level. It should be noted that, at $T = 0$, formula (21) is valid only for $x_{li} < \varepsilon_F$, otherwise, $n_{li} = 0$ (the index i numbers different local states). In the single-layer undoped graphene, the Fermi level is $E_F = 0$. Therefore, at zero temperature, only the contribution of the local level lying below the continuum band should be taken into account in the second term in relationship (19).

[1] If we go beyond the Hartree–Fock theory and consider the dynamic aspect of the problem, it can be demonstrated that the resultant spin moment on the adatom is suppressed as a result of the virtual electronic transitions adatom–substrate that occur with spin flip (Kondo effect).

For a further analysis, it is convenient to have an analytical (even if approximate) expression for the contribution n_b. This expression can be derived in the following way. The shift function is approximated by the relationship

$$\lambda(x) = \begin{cases} -a_1, & -3 < x < -1 \\ a_2, & -1 < x < 0 \\ -a_2, & 0 < x < 1 \\ a_1, & 1 < x < 3, \end{cases} \quad (22)$$

where a_1 and a_2 are positive constants determined from the condition

$$(d-1)a_1 = \int_1^d \lambda(x)dx, \quad a_2 = \int_0^1 \lambda(x)dx. \quad (23)$$

The direct calculations lead to $a_1 = 1.39$ and $a_2 = 0.77$.

By using approximation (22), we set $n_b = I(\eta_a, \gamma)$ and represent this integral in the form

$$I(\eta_a, \gamma) = I_1(\eta_a, \gamma) + I_2(\eta_a, \gamma), \quad (24)$$

$$I_1(\eta_a, \gamma) = -\gamma \int_{-3}^{-1} \frac{xdx}{(x-\eta_{a1})^2 x^2 + \pi^2\gamma^2}, \quad (25)$$

$$I_2(\eta_a, \gamma) = -\gamma \int_{-1}^{0} \frac{xdx}{(x-\eta_{a2})^2 + \pi^2\gamma^2 x^2}, \quad (26)$$

where

$$\eta_{a1,2} = \eta_a \mp \gamma a_{1,2}. \quad (27)$$

The explicit expressions for the integrals $I_1 = I_{11} + I_{12}$ and I_2 are given in Appendix 2.

The results of the numerical analysis of the band contribution n_b to the occupation number of the adatom together with the results of the approximation are presented in Fig. 4. A comparison of the results shows that the approximation proposed in our work is completely adequate at small values of the parameter γ and reproduces all specific features of the dependence of η_b on η_a (Fig. 4a). However, with an increase in the parameter γ, the approximation works well only outside the range of the adatom density-of-states specific features near the Fermi level (compare Figs. 3 and 4b, 4c), whereas, in the range of these features, the exact calculations smooth peaks given by the approximation.

Now, we turn to the calculation of the contribution of the localized states to the occupation number (19). From expression (10), we obtain

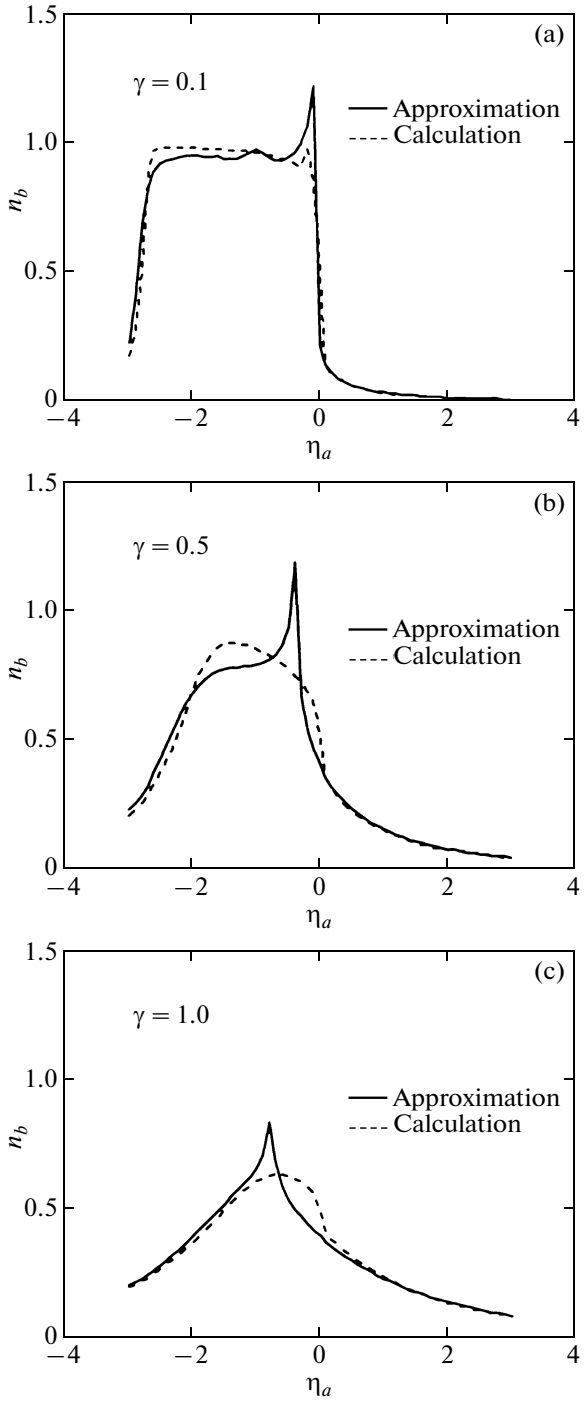

Fig. 4. Dependences of the band contribution n_b to the occupation number n_a on the position of the level of the adatom η_a with respect to the Fermi level taken as the origin for the parameters γ = (a) 0.1, (b) 0.5, and (c) 1.0.

$$\frac{d\lambda(x)}{dx} = \ln\left(\frac{x^2}{x^2-1}\right) - \frac{1}{x^2}\ln\left(\frac{x^2-1}{(x/d)^2-1}\right) - \frac{2}{x^2-d^2}, \quad (28)$$

where $|x| > d$. It is easy to see that, at $x \longrightarrow d$, we have $n_l \longrightarrow 0$. It should also be noted that, at $x \longrightarrow 0$, we

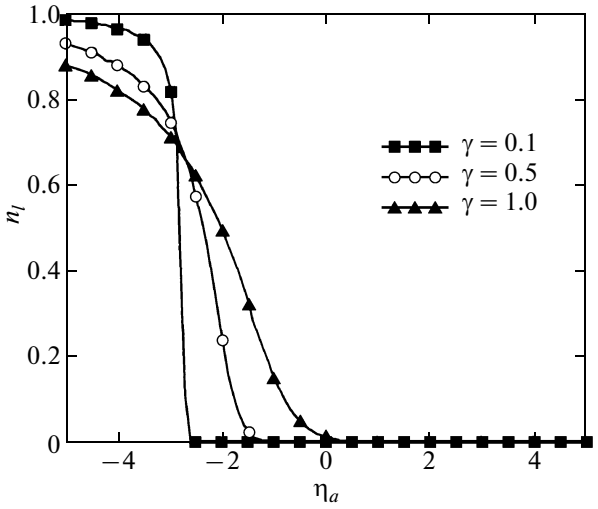

Fig. 5. Dependences of the occupation number of the local state n_l on the position of the level of the adatom η_a for the parameters $\gamma = 0.1$, 0.5, and 1.0.

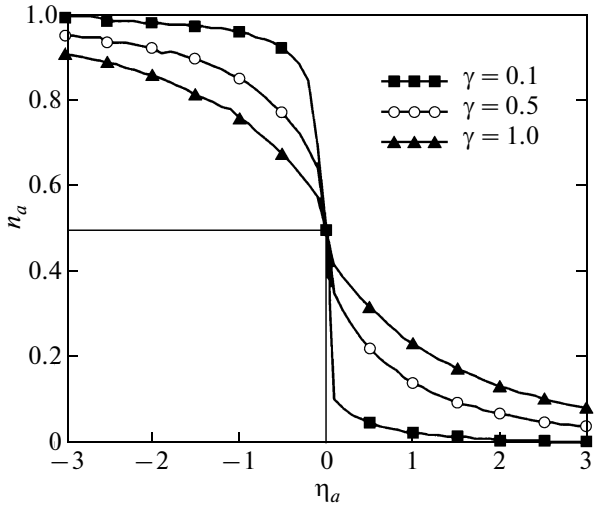

Fig. 6. Dependences of the total occupation number $n_a = n_b + n_l$ on the position of the level of the adatom η_a for the parameters $\gamma = 0.1$, 0.5, and 1.0.

find $n_l \longrightarrow 0$, because $(d\lambda/dx)_{x\to 0} \longrightarrow 2\ln|x| + 1 + 1/d^2 \longrightarrow -\infty$. The dependences of the occupation of the local level n_l of the adatom on the position η_a are plotted in Fig. 5. It was noted above that, as the local level approaches the edges of the continuum, the quantity n_l decreases sharply to zero. The dependences of the total charge of the adatom $n_a = n_b + n_l$ on η_a are shown in Fig. 6. It can be seen from this figure that an increase in the quantity η_a leads to a decrease in the occupation number of the adatom n_a. It is quite natural because the upper the position of the level of the adatom (with respect to the Fermi level), the lower its occupation. It should be emphasized that, since, at $\eta_a = 0$, the local density of states on the adatom is an even function with respect to the Fermi level, i.e., $\bar{\rho}_a(x, 0) = \bar{\rho}_a(-x, 0)$, and the local levels $\mp x_l$ are also specularly located with respect to $x = 0$, it follows from symmetry considerations that, in this case, we have $n_a = n_b + n_l = 0.5$. This circumstance can be used for verifying the correctness of the results of the calculations.

Initial data and results of the calculations for the adsorption of alkali metal atoms on the graphene

Parameter	Li	Na	K	Rb	Cs
r_a, Å	1.57	1.86	2.36	2.48	2.62
λ, Å	1.09	1.44	2.02	2.15	2.31
I, eV	5.39	5.14	4.34	4.18	3.89
η_a	1.27	1.04	1.07	1.09	1.17
V, eV	1.98	1.56	1.10	1.02	0.94
γ	0.43	0.27	0.13	0.12	0.10
Z_a (calculation)	0.90	0.92	0.96	0.96	0.97
Z_a (approximation)	0.89	0.91	0.96	0.96	0.97
V_3, eV	2.87	3.06	3.53	3.66	3.85
α_p	0.82	0.89	0.95	0.96	0.97
$\tilde{Z}$	0.82	0.89	0.95	0.96	0.97

Note: $\phi = 5.11$ eV, $a_1 = 1.39$, and $a_2 = 0.77$.

4. ADSORPTION OF ALKALI METAL IONS: EVALUATION OF THE CHARGE

Alkali metal atoms containing one electron in the outer *s* orbit are convenient objects for the verification of the applicability of the proposed model. The parameters describing these atoms are presented in the table. The values of the atomic radii r_a and the ionization energies I were taken from [39]. The center of the density of states is located by $\phi_0 = 5.11$ eV [40] below the vacuum level [41]. If the repulsion of electrons of the adatom and graphene are taken into account, it can be demonstrated [42, 43] that the *s* level of the adatom is shifted upward by $e^2/4\lambda$ (Coulomb shift), where λ is the distance from the adatom to the image plane. According to variant II proposed in [31, 32], when it is assumed that the adatom is located at the center of the hexagon, we set $\lambda = \sqrt{(r_a + r_c)^2 - d_g^2} - r_c$, where $d_g = 1.42$ Å is the distance between the nearest neighbors in the graphene and $r_c = 0.77$ Å [39]. The upward shift of the *s* level of the adatom is equivalent to a decrease in the in ionization energy $I \longrightarrow I' = I - e^2/4\lambda$. Then, we have $\eta_a = 2(\phi_0 - I')/\Delta$.

The parameter Δ can be determined using the Harrison bond-orbital method [44–46]. According to the model concepts [6, 33] and our designations (Fig. 1), we have $\Delta/2 = t$, where t is the energy (integral) of the transition between the nearest neighbors. The quantity t is set to be equal to the matrix element (taken with the opposite sign) of the energy of the π interaction between the nearest neighbors; that is,

$$-t = V_{pp\pi} = \eta_{pp\pi}\frac{\hbar^2}{m_0 d_g^2}, \qquad (29)$$

where $\eta_{pp\pi} = -0.63$ [40] and m_0 is the free-electron mass. As a result, we obtain $\Delta = 4.76$ eV ($t = 2.38$ eV). This value is in good agreement with $t = 2.7$ [47, 48] and 2.8 eV [49].

The energy V, which represents the matrix element of the σ interaction of the s orbital of the adatom and the p_z orbital of the graphene, is also determined by the Harrison method by setting

$$V = V_{sp\sigma} = \eta_{sp\sigma}\frac{\hbar^2}{m_0(r_c + r_a)^2}. \qquad (30)$$

The results of the calculations of the energy V, parameters γ, and values of n_b calculated from the formulas given in Appendix 2 are listed in the table.

Now, we evaluate the contribution of the local state appearing in the vicinity of the lower boundary of the valence band. By using relationships (17), the energy of the local state can be evaluated as $x_l'' = -d\sqrt{1 + \exp(-d\eta_a/\gamma)}$. The exponent of the exponential function is smallest for lithium, where $d\eta_a/\gamma \sim 10$. In this case, the contribution of local states is negligible, so that we can set $n_b \approx n_a = 1 - Z_a$. It follows from the table that the charge of the adatom is close to unity and increases in the series Li $\longrightarrow$ Cs, which seems to be quite natural. It should be emphasized that the data of the numerical calculations are in very good agreement with the results obtained using the approximation.

In order to quantitatively verify the results obtained, we again use the Harrison bond-orbital method and calculate the effective charge $\tilde{Z}$ on the alkali adatom–carbon atom σ bonds. For this purpose, apart from the energy V, which in the Harrison theory is referred to the covalent energy V_2, it is necessary to know the polar energy $V_3 = (\varepsilon_s - \varepsilon_p)/2$, where ε_s is the energy of the s state of the adsorbed atom and ε_p is the energy of the p state of the carbon atom. In the calculation, we set $\varepsilon_s = -I$ and $\varepsilon_p = -11.07$ eV [43, 44]. By knowing the energies V_2 and V_3, we can calculate the polarity of the bond $\alpha_p = V_3/(V_2^2 + V_3^2)^{1/2}$, which in the given case is equal to the charge of the adatom $\tilde{Z}$. All the aforementioned quantities are presented in the table. A comparison of the calculated charges Z_a and $\tilde{Z}$ indicates very good agreement, even though these charges were obtained in the framework of quite different schemes of calculations.

Unfortunately, we do not know data on the adsorption of alkali metal on the graphene. In this respect, we use the data taken from the review [50] on the adsorption on graphite. According to [50], the bond between the alkali metal atom and the graphite surface has a predominantly ionic character and the charge of the adatom increases in the series Na $\longrightarrow$ K $\longrightarrow$ Cs. As regards the charge, data of different calculations differ substantially from each other: for example, the values of Z_a for the adsorption of potassium (at its low concentrations on the surface) vary from 0.15 to 1.00 (see Table 4 in [50]). It should be noted that, in earlier works of one of the authors (S. Yu. Davydov) [31, 32], the charges Z_a equal to 0.23, 0.38, and 0.41 for Na, K, and Cs, respectively were determined in terms of the Anderson model ($\rho_g = \text{const}$) for zero coverages. The differences between the results obtained in [31, 32] and those reported in our work are associated not only with the difference in the model of the density of states of the substrate but also with the work function of the substrate: the work function in [31, 32] is $\phi_0 = 4.60$ eV for graphite [51], whereas the work function in the present work is $\phi_0 = 5.11$ eV for graphene [40]. Therefore, the solution of the problem calls for further experimental investigation.

Thus, in this work, we have proposed an M-shaped model of the density of states of graphene. This model has been used to determine the local density of states on the adatom and its occupation numbers. The proposed approximation has made it possible to adequately describe the occupation numbers in analytical way. It has been demonstrated that the M model allows one to obtain reasonable charges of adsorbed atoms of alkali metals.

APPENDIX 1

In order to explain the behavior of the central $\bar{\rho}_a(x_0)$ and side $\bar{\rho}_a(x_1)$ maxima (Fig. 3), let us consider the extrema of the function $\bar{\rho}_a(x)$ that are determined by the equation

$$\frac{df}{dx}(1 - 2\pi^2 f\gamma\bar{\rho}_a) - \frac{2\bar{\rho}_a}{\gamma}\left(1 - \gamma\frac{d\lambda}{dx}\right) = 0, \qquad (A.1.1)$$

where

$$\frac{d\lambda}{dx} = \ln\left|\frac{x^2}{1-x^2}\right| - \frac{1}{x^2}\ln\left|\frac{1-x^2}{1-(x/3)^2}\right| + \frac{2}{9-x^2}. \quad \text{(A.1.2)}$$

The position of the main maximum is sought under the assumption that $|x_0| \ll 1$. In this range, we have $f = -x$, $df/dx = -1$, $\lambda(x) \sim 2x\ln|x|$, and $d\lambda/dx \sim 2\ln|x|$. We assume that the resonance level x_r coincides with x_0. Then, we find that $\bar{\rho}_a(x_0) \sim (|x_0|\gamma\pi^2)^{-1}$. In this case, we have $(1 - 2\pi^2 f\gamma\bar{\rho}_a) \sim -1$ and it follows from Eq. (A.1.1) that $\bar{\rho}_a \propto \gamma$ (Fig. 3b for $\gamma = 0.5$ and 1.8, because only these two cases satisfy the condition $|x_0| \ll 1$). An increase in the quantity $|\eta_a|$ leads to a shift in x_0 toward higher (in magnitude) energies, which results in a decrease in the height of the main maximum of the density of states (Fig. 3a), because $\bar{\rho}_a(x_0) \propto |x_0|^{-1}$.

Now, we consider the behavior of the side maximum $\bar{\rho}_a(x_1)$. The solution of Eq. (A.1.1) is sought in the range $-3 < x < -1$, where $f = -1/x$ and $df/dx = 1/x^2$. If we again assume that the maximum $\bar{\rho}_a(x_1)$ is located in the vicinity of the resonance level $x_r \sim \eta_a - \gamma\lambda(x_r)$, we have $\bar{\rho}_a(x_1) \sim |x_1|/\pi^2\gamma$. It immediately follows that an increase in the quantity γ leads to a decrease in the maximum $\bar{\rho}_a(x_1)$ (Fig. 3b). An increase in $|\eta_a|$ results in an increase in the value of $|x_1|$, and, as a consequence, the maximum $\bar{\rho}_a(x_1)$ increases (Fig. 3a).

APPENDIX 2

In order to calculate the integral I_1, we introduce the new variable $y = x - \eta_{a1}/2$. Then, we have $x^2(x-\eta_{a1})^2 = \left(y^2 - \frac{1}{4}\eta_{a1}^2\right)^2$. The integral I_1 can be represented in the form

$$I_1 = I_{11} + I_{12}, \quad \text{(A.2.1)}$$

where

$$I_{11} = \frac{1}{2}\gamma\int_{(1+\eta_{a1}/2)^2}^{(3+\eta_{a1}/2)^2}\frac{dz}{\left(z-\frac{1}{4}\eta_{a1}^2\right)^2 + (\pi\gamma)^2}, \quad z = y^2, \quad \text{(A.2.2)}$$

$$I_{12} = -\frac{1}{2}\gamma\eta_{a1}\int_{-(3+\eta_{a1}/2)}^{-(1+\eta_{a1}/2)}\frac{dy}{\left(y^2-\frac{1}{4}\eta_{a1}^2\right)^2 + (\pi\gamma)^2}. \quad \text{(A.2.3)}$$

By using standard integrals [52], we find

$$I_{11} = \frac{1}{2\pi}\left(\arctan\frac{3(3+\eta_{a1})}{\pi\gamma} - \arctan\frac{1+\eta_{a1}}{\pi\gamma}\right), \quad \text{(A.2.4)}$$

$$I_{12} = -\frac{\mathrm{sgn}(\eta_{a1})}{4\pi(1+\beta^2)^{1/4}} \times\left[\sin(\alpha/2)\ln\left(\frac{g_{1-}g_{3+}}{g_{1+}g_{3-}}\right) + 2\cos(\alpha/2)(H_3 - H_1)\right], \quad \text{(A.2.5)}$$

$$H_1 = \arctan(h_1) + \pi\theta\left(-1-\frac{1}{2}\eta_{a1}\right),$$
$$H_3 = \arctan(h_3) + \pi\theta\left(-3-\frac{1}{2}\eta_{a1}\right), \quad \text{(A.2.6)}$$

where

$$Q(z) = \begin{cases}1, & z>0\\ 0, & z<0,\end{cases}$$
$$\mathrm{sgn}(\xi) = 1 \quad \text{at} \quad \xi > 0 \quad \text{(A.2.7)}$$
$$\text{and} \quad \mathrm{sgn}(\xi) = -1 \quad \text{at} \quad \xi < 0,$$

$$g_{1\pm} = \left(1+\frac{1}{2}\eta_{a1}\right)^2 \pm 2q\cos(\alpha/2)\left(1+\frac{1}{2}\eta_{a1}\right) + q^2,$$

$$h_1 = \frac{\left(1+\frac{1}{2}\eta_{a1}\right)^2 - q^2}{2q\sin(\alpha/2)\left(1+\frac{1}{2}\eta_{a1}\right)},$$
$$h_3 = \frac{\left(3+\frac{1}{2}\eta_{a1}\right)^2 - q^2}{2q\sin(\alpha/2)\left(3+\frac{1}{2}\eta_{a1}\right)}, \quad \text{(A.2.8)}$$

$$\sin(\alpha/2) = \sqrt{\frac{1}{2}(1-\cos\alpha)},$$
$$\cos(\alpha/2) = \sqrt{\frac{1}{2}(1+\cos\alpha)}, \quad \cos\alpha = \frac{1}{\sqrt{1+\beta^2}}, \quad \text{(A.2.9)}$$

$$q = \frac{1}{2}|\eta_{a1}|(1+\beta^2)^{1/4}, \quad \text{(A.2.10)}$$

$$\beta = \frac{4\pi\gamma}{\eta_{a1}^2}. \quad \text{(A.2.11)}$$

We again use standard integrals [52] and find that the integral I_2 is represented by the expression ($\eta_{a2} \neq 0$)

$$I_2 = \frac{\gamma}{2(1+(\pi\gamma)^2)}\left[\ln\frac{(1+\eta_{a2})^2 + (\pi\gamma)^2}{\eta_{a2}^2} + \frac{2}{\pi\gamma}\left(\arctan\frac{1}{\pi\gamma} - \arctan\frac{1+\eta_{a2}+(\pi\gamma)^2}{|\eta_{a2}|\pi\gamma}\right)\right]. \quad \text{(A.2.12)}$$

It should be noted that the theta function in relationship (A.2.6) provides the continuity of arctangents with a variation in the parameter η_{a1}.

ACKNOWLEDGMENTS

This study was supported by the Presidium of the Russian Academy of Sciences (Programs "Quantum Physics of Condensed Matter" and "Principles of Basic Research of Nanotechnologies and Nanomaterials"), the Federal Agency for Science and Innovation of the Russian Federation (contract no. 02.740.11.0108), the Branch of Physical Sciences of the Russian Academy of Sciences ("New Materials"), and the Ministry of Education and Science of the Russian Federation (Federal Target Program "Development of the Scientific Potential of the Higher School (2009–2010)," project no. 2.1.1/2503).

REFERENCES

1. Yu. S. Nechaev and O. K. Alekseeva, Usp. Khim. **73**, 1308 (2004).
2. M. Caragin and S. Finberg, J. Phys.: Condens. Matter **17**, R995 (2005).
3. Yu. S. Nechaev, Usp. Fiz. Nauk **176** (6), 581 (2006) [Phys.—Usp. **49** (6), 563 (2006)].
4. S. V. Bulyarskii and A. S. Basaev, Zh. Eksp. Teor. Fiz. **135** (4), 788 (2009) [JETP **108** (4), 688 (2009)].
5. A. K. Geim and K. S. Novoselov, Nat. Mater. **6**, 183 (2007).
6. A. H. Castro Nero, F. Guinea, N. M. R. Peres, K. S. Novoselov, and A. K. Geim, Rev. Mod. Phys. **81**, 109 (2009).
7. V. V. Cheianov, O. Siljuäsen, B. L. Alshuler, and V. Fal'ko, Phys. Rev. B: Condens. Matter **80**, 233409 (2009).
8. Y.-H. Lu, L. Chi, and Y.-P. Feng, Phys. Rev. B: Condens. Matter **80**, 233410 (2009).
9. J. Dai, J. Yuan, and P. Giannozzi, Appl. Phys. Lett. **95**, 232105 (2009).
10. H. McKay, D. J. Wales, S. J. Jenkins, J. A. Verges, and P. L. de Andres, Phys. Rev. B: Condens. Matter **81**, 075425 (2009).
11. M. Klintenberg, S. Lebergue, M. I. Katsnelson, and O. Eriksson, ArXiv:1001.3829.
12. V. V. Cheianov, O. Siljuäsen, B. L. Altshuler, and V. Fal'ko, ArXiv:1002.2330.
13. A. N. Rudenko, F. J. Keil, M. I. Katsnelson, and A. I. Lichtenstein, ArXiv:1002.2536.
14. A. Saffarzadeh, ArXiv:1002.3941.
15. J. Soltys, J. Piechota, M. Lopuszynski, and S. Krukowski, ArXiv:1002.4717.
16. F. Schedin, A. K. Gaim, S. V. Morozov, E. W. Hill, P. Blake, M. I. Katsnelson, and K. S. Novoselov, Nat. Mater. **6**, 652 (2007).
17. T. O. Wehling, K. S. Novoselov, S. V. Morozov, E. E. Vdovin, M. I. Katsnelson, A. K. Geim, and A. I. Lichtenstein, Nano Lett. **8**, 173 (2008).
18. H. E. Romero, P. Joshi, A. K. Gupta, H. R. Gutierrez, M. W. Cole, S. A. Tadigadapa, and P. C. Eklund, Nanotechnology **6**, 652 (2007).
19. G. Lu, L. E. Ocola, and J. Chen, Nanotechnology **20**, 445502 (2009).
20. H. Pinto, R. Jones, J. P. Gross, and P. R. Briddon, ArXiv:1003.0624.
21. D. M. Newns, Phys. Rev. **178**, (3), 1123 (1969).
22. P. W. Anderson, Phys. Rev. **124** (1), 41 (1961).
23. L. A. Bol'shov, A. P. Napartovich, A. G. Naumovets, and A. G. Fedorus, Usp. Fiz. Nauk **122** (1), 125 (1977) [Sov. Phys.—Usp. **20** (5), 432 (1977)].
24. O. M. Braun, Ukr. Fiz. Zh. **23** (8), 1233 (1978).
25. O. M. Braun and V. K. Medvedev, Usp. Fiz. Nauk **157** (4), 631 (1989) [Sov. Phys.—Usp. **32** (4), 328 (1989)].
26. F. D. M. Haldane and P. W. Anderson, Phys. Rev. B: Solid State **13** (6), 2553 (1976).
27. S. Yu. Davydov and S. V. Troshin, Fiz. Tverd. Tela (St. Petersburg) **49** (8), 1508 (2007) [Phys. Solid State **49** (8), 1583 (2007)].
28. S. Yu. Davydov, Fiz. Tverd. Tela (St. Petersburg) **51** (4), 803 (2009) [Phys. Solid State **51** (4), 849 (2009)].
29. S. Yu. Davydov, Fiz. Tekh. Poluprovodn. (St. Petersburg) **43** (7), 865 (2009) [Semiconductors **43** (7), 833 (2009)].
30. S. Yu. Davydov, Fiz. Tekh. Poluprovodn. (St. Petersburg) **31** (10), 1236 (1997) [Semiconductors **31** (10), 1062 (1997)].
31. S. Yu. Davydov, Pis'ma Zh. Tekh. Fiz. **35** (18), 28 (2009) [Tech. Phys. Lett. **35** (9), 847 (2009)].
32. S. Yu. Davydov, Pis'ma Zh. Tekh. Fiz. **35** (21), 50 (2009) [Tech. Phys. Lett. **35** (11), 998 (2009)].
33. P. R. Wallace, Phys. Rev. **71** (9), 622 (1947).
34. C. A. Coulson and R. Taylor, Proc. Phys. Soc., London, Sect. A **65**, 815 (1952).
35. J. W. McClure, Phys. Rev. **108** (3), 612 (1957).
36. B. Ahuja, S. Auluck, J. Trigg, J. M. Wills, O. Eriksson, and B. Johansson, Phys. Rev. B: Condens. Matter **51** (8), 4813 (1995).
37. V. Kapko, D. A. Drabold, and M. F. Thorpe, ArXiv:0912.0729.
38. C. Bena and S. A. Kivelson, Phys. Rev. B: Condens. Matter **72**, 125432 (2005).
39. *Handbook of Physical Quantities*, Ed. by I. S. Grigoriev and E. Z. Meilikhov (Energoatomizdat, Moscow, 1991; CRC Press, Boca Raton, Florida, United States, 1997).
40. A. Mattausch and O. Pankratov, Phys. Rev. Lett. **99**, 076802 (2007).
41. G. S. Painter and D. E. Ellis, Phys. Rev. B: Solid State **1**, 12, 4747 (1970).
42. J. W. Gadzuk, Phys. Rev. B: Solid State **1** (5), 2110 (1970).
43. T. L. Einstein, J. A. Hertz, and J. R. Schrieffer, in *Theory of Chemisorption*, Ed. by J. Smith (Springer, Heidelberg, 1980; Mir, Moscow, 1983).
44. W. Harrison, *Electronic Structure and Properties of Solids* (Freeman, San Francisco, California, United States, 1980; Mir, Moscow, 1983), Vol. 1.
45. W. A. Harrison, Phys. Rev. B: Condens. Matter **27** (6), 3592 (1983).

46. W. A. Harrison, Phys. Rev. B: Condens. Matter **31** (4), 2121 (1985).

47. M. Ezawa, ArXiv:1003.1766v1 (2010).

48. S. Wu and F. Lin, ArXiv:1001.2057v1 (2010).

49. W. Li and R. Tao, ArXiv:1001.4168v1 (2010).

50. M. Caragiu and S. Finberg, J. Phys.: Condens. Matter **17** (35), R995 (2005).

51. M. Breitgolz, J. Algdal, T. Kihlgren, and S.-A. Lindgren, Phys. Rev. B: Condens. Matter **70**, 125108 (2004).

52. I. S. Gradshteyn and I. M. Ryzhik, *Table of Integrals, Series, and Products* (Nauka, Moscow, 1971; Academic, London, 1994).

Translated by O. Borovik-Romanova